

Article

The Different Metabolic Responses of Resistant and Susceptible Wheats to *Fusarium graminearum* Inoculation

Caixiang Liu ^{1,2,†} , Fangfang Chen ^{3,4,†}, Laixing Liu ⁵, Xinyu Fan ⁶, Huili Liu ^{1,2}, Danyun Zeng ^{1,2} and Xu Zhang ^{1,2,7,*}

- ¹ State Key Laboratory of Magnetic Resonance and Atomic and Molecular Physics, National Center for Magnetic Resonance in Wuhan, Wuhan Institute of Physics and Mathematics, Innovation Academy for Precision Measurement of Science and Technology, Chinese Academy of Sciences, Wuhan 430071, China
- ² University of Chinese Academy of Sciences, Beijing 100049, China
- ³ Songjiang Yujian High School affiliated to Shanghai Foreign Language School, Shanghai 201600, China
- ⁴ Molecular Biotechnology Laboratory of Triticeae Crops, Huazhong Agricultural University, Wuhan 430070, China
- ⁵ School of Management Wuhan Institute of Technology, Wuhan 430205, China
- ⁶ State Key Laboratory of Component-based Chinese Medicine, Tianjin University of Traditional Chinese Medicine, Tianjin 300193, China
- ⁷ Wuhan National Laboratory for Optoelectronics, Huazhong University of Science and Technology, Wuhan 430074, China
- * Correspondence: zhangxu@apm.ac.cn; Tel.: +86-27-87197056; Fax: +86-27-87199291
- † These authors contributed equally to this work.



Citation: Liu, C.; Chen, F.; Liu, L.; Fan, X.; Liu, H.; Zeng, D.; Zhang, X. The Different Metabolic Responses of Resistant and Susceptible Wheats to *Fusarium graminearum* Inoculation. *Metabolites* **2022**, *12*, 727. <https://doi.org/10.3390/metabo12080727>

Academic Editors: Tae-Hwan Kim, Cécile Vriet and Luis Gómez

Received: 5 July 2022

Accepted: 31 July 2022

Published: 6 August 2022

Publisher's Note: MDPI stays neutral with regard to jurisdictional claims in published maps and institutional affiliations.



Copyright: © 2022 by the authors. Licensee MDPI, Basel, Switzerland. This article is an open access article distributed under the terms and conditions of the Creative Commons Attribution (CC BY) license (<https://creativecommons.org/licenses/by/4.0/>).

Abstract: *Fusarium* head blight (FHB) is a serious wheat disease caused by *Fusarium graminearum* (Fg) Schwabe. FHB can cause huge loss in wheat yield. In addition, trichothecene mycotoxins produced by Fg are harmful to the environment and humans. In our previous study, we obtained two mutants *TPS1*[−] and *TPS2*[−]. Neither of these mutants could synthesize trehalose, and they produced fewer mycotoxins. To understand the complex interaction between Fg and wheat, we systematically analyzed the metabolic responses of FHB-susceptible and -resistant wheat to ddH₂O, the *TPS*[−] mutants and wild type (WT) using NMR combined with multivariate analysis. More than 40 metabolites were identified in wheat extracts including sugars, amino acids, organic acids, choline metabolites and other metabolites. When infected by Fg, FHB-resistant and -susceptible wheat plants showed different metabolic responses. For FHB-resistant wheat, there were clear metabolic differences between inoculation with mutants (*TPS1*[−]/*TPS2*[−]) and with ddH₂O/WT. For the susceptible wheat, there were obvious metabolic differences between inoculation with mutant (*TPS1*[−]/*TPS2*[−]) and inoculation with ddH₂O; however, there were no significant metabolic differences between inoculation with *TPS*[−] mutants and with WT. Specifically, compared with ddH₂O, resistant wheat increased the levels of Phe, p-hydroxy cinnamic acid (p-HCA), and chlorogenic acid in response to *TPS*[−] mutants; however, susceptible wheat did not. Shikimate-mediated secondary metabolism was activated in the FHB-resistant wheat to inhibit the growth of Fg and reduce the production of mycotoxins. These results can be helpful for the development of FHB-resistant wheat varieties, although the molecular relationship between the trehalose biosynthetic pathway in Fg and shikimate-mediated secondary metabolism in wheat remains to be further studied.

Keywords: *Fusarium graminearum*; resistant and susceptible wheat; trehalose biosynthesis; *TPS1*[−]; *TPS2*[−]; metabonomics; NMR

1. Introduction

Fusarium head blight (FHB) is one of the most devastating diseases of wheat (*Triticum aestivum* L.) globally. FHB, caused by *Fusarium graminearum* (Fg) Schwabe (teleomorph *Gibberella zeae* Petch), not only leads to huge reductions in wheat grain yield, but also harms the environment and humans by producing deteriorated grain quality contaminated

with trichothecene mycotoxins [1–4]. Since 1993, FHB has become a major problem for the agriculture industry in North America [5,6]. Apart from FHB, *Fg* can also infect other cereals (such as barley, maize, and oats), and cause stalk rot or root rot [7]. Although fungicides have been applied to control *Fg*, the resulting environmental problems and fungicide resistance are not negligible [7]. Breeding FHB-resistant wheat varieties is considered to be an economical and environmentally friendly approach to managing FHB.

Trehalose is a nonreducing disaccharide formed by two glucose molecules linked with a 1 α –1 α bond, and is widely found in plants, bacteria, fungi and insects [8]. In recent years, trehalose has drawn considerable attention for its important functions in serving as a carbon source [9], regulating osmotic pressure as a compatible solute in prokaryotes [10], and stabilizing and protecting membranes and proteins [11,12]. In addition, trehalose plays a significant role in the response to various stresses such as oxidative stress, heat, and drought [13–15]. More importantly, trehalose may play a role in signaling or regulation [16].

It is reported that there are at least five pathways for trehalose biosynthesis in different organisms [8,16]. The best-known pathway involves two steps: the first step is being catalyzed by trehalose 6-phosphate synthase (TPS1), and the second step is being catalyzed by trehalose 6-phosphate phosphatase (TPS2). TPS1 catalyzes the transfer of combined uridinediphospho (UDP) glucose and glucose 6-phosphate to generate trehalose 6-phosphate (T6P), while TPS2 is responsible for catalyzing the dephosphorylation of T6P to form trehalose [17,18]. Many studies have demonstrated that, apart from involvement in trehalose synthesis, *TPS* genes also take part in the development, pathogenicity and stress responses in yeast and higher fungi [19]. Blocking trehalose synthesis may be a promising approach for managing fungal diseases [20].

We obtained two mutant strains, *TPS1*[−] and *TPS2*[−], from our previous study, carrying a single deletion of *TPS1* or *TPS2*, respectively [21]. The results showed that *TPS1* appeared unessential for *Fg* development and virulence, while *TPS2* deletion abolished sporulation and sexual reproduction of *Fg*. In addition, it was reported that the *TPS2*[−] mutant had a more significant reduction in the production of mycotoxins compared with the *TPS1*[−] mutant [22].

Metabonomics has emerged as a powerful tool for studying the metabolic responses of plants to both biotic and abiotic stresses [23–29]. It has been used in understanding the interaction between plants and pathogens [30,31] and between plants and insects [24,32,33]. For example, metabolomics analysis of wheat leaves and stem tissues indicated that the levels of betaine, sucrose, glucose, glutamate, glutamine, alanine, trans-aconitic acid, and some aromatic compounds were positively correlated with FHB resistance [34]. Moreover, Liu et al. [25] found that the activation of γ - amino butyric acid shunt and shikimate-mediated secondary metabolism was vital for rice plants to resist insect infestation. Furthermore, combined transcriptomic and metabolomic analyses revealed that the tryptophan synthesis pathway plays an important role in the resistance of cotton to *V. dahlia* [35]. So far, the metabolic responses of FHB-resistant and -susceptible wheat to *TPS*[−] mutants and WT is unclear. However, this information can afford us metabolites or metabolic pathways related to FHB resistance and can afford help in controlling *Fg* and developing FHB-resistant wheat varieties.

In this study, we analyzed the metabolomics profiles of FHB-resistant and -susceptible wheat varieties inoculated with ddH₂O, WT, and *TPS*[−] mutants. Our objectives are to obtain the different metabolic responses of resistant and susceptible wheat to ddH₂O, WT, and *TPS*[−] mutants, which will offer important information for further cultivating FHB-resistant wheat varieties.

2. Materials and Methods

2.1. Chemicals

Methanol, NaH₂PO₄·2H₂O, and K₂HPO₄·3H₂O were purchased from Guoyao Chemical Co. Ltd. (Shanghai, China), while sodium 3-trimethylsilyl [2, 2, 3, 3-D₄] propionate (TSP) and D₂O (99.9% D) were obtained from Cambridge Isotope Laboratory (Miami, FL, USA).

2.2. Fungus Material Culture and Plant Materials

Fg strain 5035 (wild type, WT) was isolated from a scabby wheat spike in Wuhan (China). Strain 5035 was highly pathogenic to wheat through producing many mycotoxins [36,37]. *TPS1*[−] and *TPS2*[−] are two isogenic strains obtained from homologous recombination of *Fg* strain 5035 through *Agrobacterium*-mediated transformation [21]. Molecular characterization confirmed that trehalose 6-phosphate synthase gene was deleted in the *TPS1*[−] mutant, while trehalose 6-phosphate phosphatase was deleted in the *TPS2*[−] mutant [21]. *Fg* strains were cultured in CMC broth (7.5 g/L of carboxymethyl cellulose, 0.5 g/L of KH₂PO₄, 0.5 g/L of NH₄NO₃, 0.25 g/L of MgSO₄·7H₂O, and 0.5 g/L of yeast extract) [38] at 28 °C for 5 days (200 rpm). Conidiospores were collected and adjusted to the concentration of about 1 × 10⁶ spores/mL, and 10 μL of the conidia was cultured at 28 °C on potato-dextrose agar (PDA) for 3 days.

In this experiment, the wheat variety Sumai 3, which is resistant to FHB, and Annong 8455, which is susceptible to FHB, were grown in fields at Huazhong Agricultural University, Wuhan, China [39]. At the early anthesis, one spike per wheat was inoculated with 10 μL of ddH₂O or the above conidia suspensions (*Fg* WT, *TPS1*[−], and *TPS2*[−]) using a pipette tip for 96 h. Five inoculated spikes were collected as a sample, and a total of 46 samples of the two wheat varieties were obtained to afford five to seven biological replicates (n = 5–7). The wheat spikes were harvested and snap-frozen in liquid nitrogen, then stored at −80 °C until further analysis.

2.3. Metabolite Extraction for Wheat

Metabolites in wheat spikes were extracted using a previously reported method with some improvements [24]. The samples were freeze-dried, ground into powder with a mortar and pestle, and about 25 mg of the powder samples was transferred into a 2 mL Eppendorf tube with the addition of 1.2 mL of methanol/water solution (*v/v* = 2/1, −40 °C) and one 5 mm tungsten carbide bead (Qiagen, Germany). The mixture was homogenized using a tissuelyser (Qiagen, Germany) after drastically vortexing for 30 s followed by 15 min intermittent sonication (i.e., 30 s sonication with 30 s break) in an ice bath. The supernatant of each sample was transferred into a new 5 mL Eppendorf tube following centrifugation for 10 min (16,099 × *g*, 4 °C). The remaining residues were further extracted twice using the same method, and three supernatants were combined as one sample. After removal of methanol under vacuum, samples were lyophilized. The freeze-dried extracts were redissolved in 600 μL of phosphate buffer (0.1 M K₂HPO₄-NaH₂PO₄, pH 7.4) containing 50% D₂O (*v/v*) and 0.02% TSP [40]. After being centrifuged for 10 min (16,099 × *g*, 4 °C), a total of 500 μL of supernatant for each sample was transferred into 5 mm NMR tubes for NMR-based metabolite analysis.

2.4. NMR Measurements

All ¹H NMR spectra of samples for wheat spikes were acquired at 298 K using an inverse detection cryogenic probe on a Bruker AVIII 600 spectrometer (Bruker Biospin, GmbH, Rheinstetten, Germany). The ¹H NMR spectra were acquired using NOESY pulse sequence (RD-90°-t1-90°-tm-90°-acquisition) with 90° pulse length of about 9.4 μs and t1 was set to 2 μs. Water peak was saturated with a weak irradiation during the recycle delay (RD) of 2 s and a mixing time (tm) of 100 ms, and 32 transients were collected into 64 k data points with a spectral width of 20 ppm. A series of ²D NMR spectra including ¹H-¹H TOCSY, ¹H-¹H COSY, ¹H-JRES, ¹H-¹³C HSQC, and ¹H-¹³C HMBC spectra were acquired using selected samples for metabolite assignments [24].

2.5. Spectral Processing and Multivariate Data Analysis

Following phase and baseline correction using TopSpin (v3.1, Bruker Biospin GmbH, Germany), all NMR spectra were referenced to the internal standard TSP at δ 0.000 ppm. The spectral region between 0.5 and 10.0 ppm was divided into bins with a width of 0.004 ppm (2.4 Hz) using the AMIX software (v 3.8.3, Bruker Biospin GmbH, Germany).

The water regions at δ 4.700–5.100 were removed. A total of 2275 bins for all remaining regions were normalized to the dry weight of wheat spikes to give a dataset in the form of signal area (metabolite quantity) per gram dry weight of wheat.

Principal component analysis (PCA) and orthogonal projection to latent structures discriminant analysis (OPLS-DA) [41] were both performed on the normalized NMR data using SIMCA-P+ software (v12.0, Umetrics, Umea, Sweden). In OPLS-DA models, one orthogonal and one predictive component were calculated using the unit-variance (UV) scaled NMR data as X-matrix and the class information as Y-matrix. The model qualities were described by the explained variances for X-matrix (R^2X values) and the model predictability (Q^2 values) with further assessment with ANOVA of the cross-validated residuals (CV-ANOVA) approach where intergroup differences were considered as significant with p value < 0.05 [42]. Leave-One-Out (LOO) validation was used in the cross-validation of the models. The results were exhibited in both the form of scores plots and loadings plots, in which scores plots and loadings plots showed group clustering and indicated variables (metabolite levels) contributing to inter-group differences, respectively. In such loading plots, variables were color-coded according to absolute values of the correlation coefficients ($|r|$) [43], and variables (i.e., metabolite contents) with a cool color (e.g., blue) showed less significant contributions to inter-group differences than those with a warm color (e.g., red). In this study, the metabolites showing statistically significant changes were obtained at the level of $p < 0.05$.

3. Results

3.1. Metabolic Profiles for FHB-Susceptible and -Resistant Wheats

^1H NMR spectra of wheat spike extracts showed obvious difference in the metabolic profiles for FHB-resistant wheat (Sumai 3) inoculated with ddH₂O, WT, *TPS1*[−], and *TPS2*[−] (Figure 1). Similarly, there was also an obvious difference in the metabolic profiles for the FHB-susceptible wheat (Annong 8455) inoculated with ddH₂O, WT, *TPS1*[−], and *TPS2*[−] (Figure 2). Signals were assigned to individual metabolites (Table S1) based on data in the literature [23,44,45] and in-house databases. A series of 2D NMR spectra were acquired for selected samples to further confirm metabolite identifications. More than 40 metabolites were identified, including 5 sugars (sucrose, glucose, raffinose, fructose, and myo-inositol), 16 amino acids and their metabolites (Val, Ieu, Ile, Thr, Ala, Arg, Met, GABA, Glu, Gln, Asp, Asn, Phe, Trp, Tyr, and His), 9 organic acids (acetate, lactate, pyruvate, succinate, fumarate, citrate, α -ketoglutarate, malate, and formate), 5 choline metabolites (choline, phosphocholine, glycine betaine, ethanolamine, and dimethylglycine), 6 nucleotide metabolites (adenosine, uridine, guanosine, hypoxanthine, inosine, and AMP), and 2 secondary metabolites (*p*-hydroxy cinnamic acid and chlorogenic acid) (Figures 1 and 2, Table S1).

Visual inspection of Figure 1 suggested that for the resistant wheat Sumai 3, inoculation with the *TPS1*[−] mutant for 96 h induced significant elevation in guanosine level along with a decrease in α -ketoglutarate level when compared with inoculation with ddH₂O, and it had decreases in myo-inositol and Asp levels when compared with inoculation with WT (Figure 1a–c). In addition, for the resistant wheat Sumai 3, inoculation with the *TPS2*[−] mutant induced significantly higher levels of Phe and chlorogenic acid than inoculation with ddH₂O, and it had a lower level of sucrose than with inoculation with WT (Figure 1a,b,d).

For the susceptible wheat variety Annong 8455, the level of adenosine was higher in response to inoculation with the *TPS1*[−] mutant for 96 h than inoculation with ddH₂O, and the levels of sucrose and guanosine were lower after being inoculated with the *TPS2*[−] mutant compared with inoculation with ddH₂O (Figure 2). Moreover, inoculation with the *TPS2*[−] mutant induced a more significant reduction in glucose and malate levels in the susceptible wheat than inoculation with the *TPS1*[−] mutant (Figure 2c,d). To obtain more detailed information about metabolic changes in the resistant and susceptible wheats induced by ddH₂O, WT, *TPS1*[−], and *TPS2*[−], multivariate data analyses were performed on the NMR data of these wheat spikes.

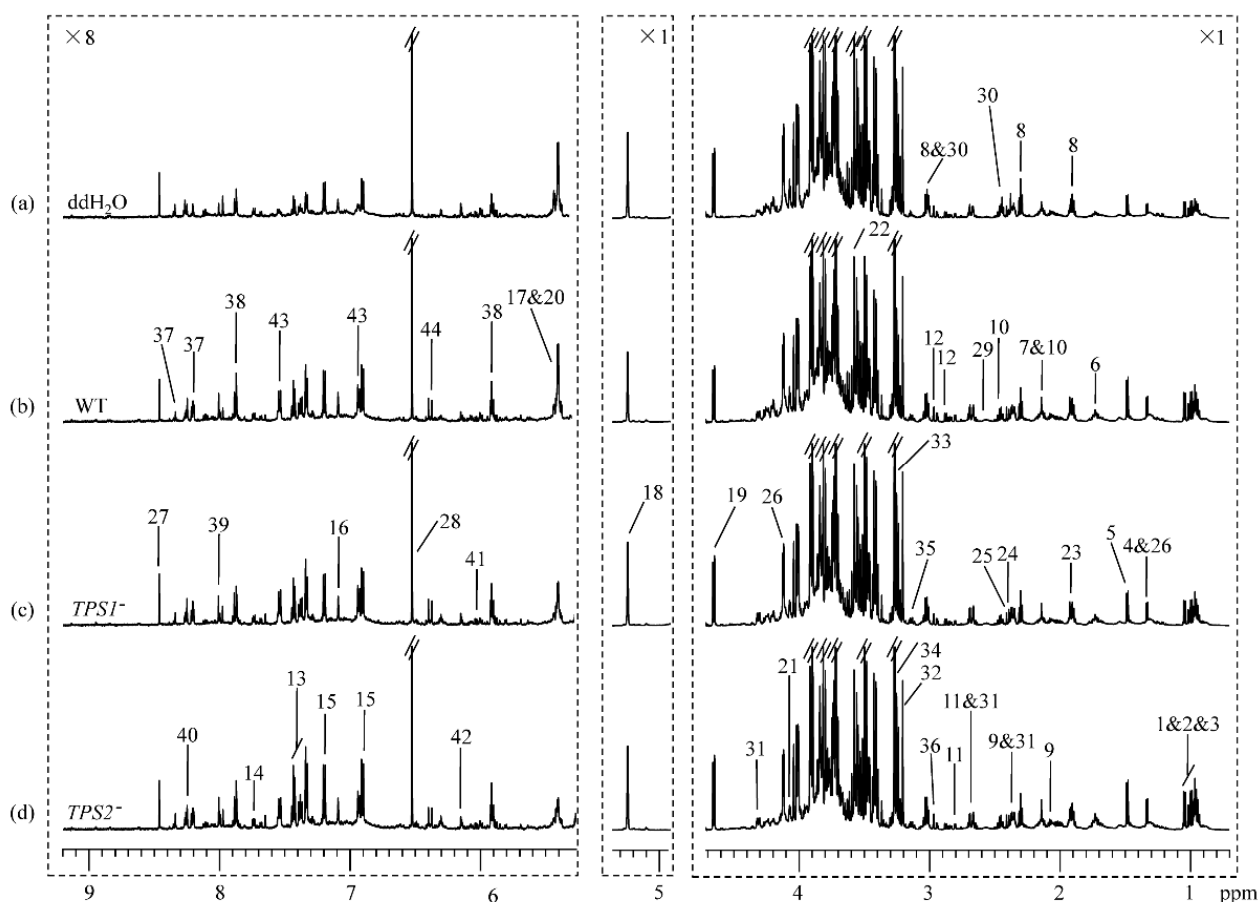


Figure 1. ^1H NMR spectra of extracts for resistant wheat Sumai 3 inoculated with (a) ddH_2O , (b) *Fg* WT 5035, (c) *Fg* TPS1^- mutant, and (d) *Fg* TPS2^- mutant for 96 h. The region δ 5.31–9.21 was vertically expanded 8 times. Keys: 1, isoleucine (Ile); 2, leucine (Leu); 3, valine (Val); 4, threonine (Thr); 5, alanine (Ala); 6, arginine (Arg); 7, methionine (Met); 8, γ -aminobutyrate (GABA); 9, glutamate (Glu); 10, glutamine (Gln); 11, aspartate (Asp); 12, asparagine (Asn); 13, phenylalanine (Phe); 14, tryptophan (Trp); 15, tyrosine (Tyr); 16, histidine (His); 17, sucrose; 18, α -glucose; 19, β -glucose; 20, raffinose; 21, fructose; 22, myo-inositol; 23, acetate; 24, pyruvate; 25, succinate; 26, lactate; 27, formate; 28, fumarate; 29, citrate; 30, α -ketoglutarate (α -KG); 31, malate; 32, choline; 33, phosphocholine (PC); 34, glycine betaine (GB); 35, ethanolamine (EA); 36, dimethylamine; 37, adenosine; 38, uridine; 39, guanosine; 40, hypoxanthine; 41, inosine; 42, deoxy adenosine monophosphate (dAMP); 43, p-hydroxy cinnamic acid; 44, chlorogenic acid; 45, thymidine.

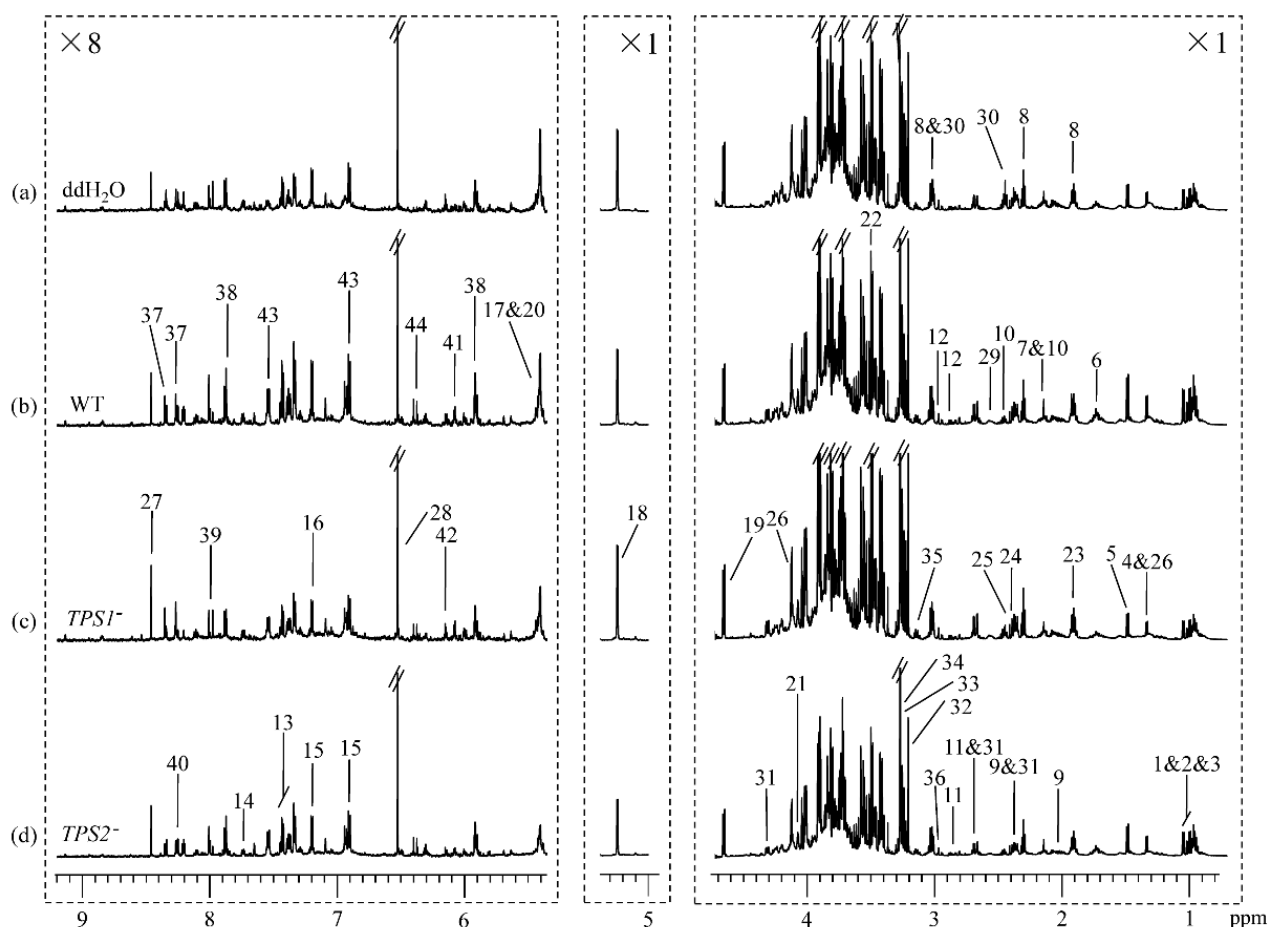


Figure 2. ^1H NMR spectra of extracts for susceptible wheat Anong 8455 inoculated with (a) ddH_2O , (b) *Fg* WT 5035, (c) *Fg* TPS1^- mutant, and (d) *Fg* TPS2^- mutant for 96 h. The region δ 5.31–9.21 was vertically expanded 8 times. Keys were indicated in Figure 1 and Table S1.

3.2. Different Metabolic Responses of FHB-Resistant and -Susceptible Wheats to Three *Fusarium* Strains

PCA of the NMR data for FHB-resistant and -susceptible wheat spikes showed that there were no obvious metabolic differences between those inoculated with mutants (including TPS1^- and TPS2^-) and those inoculated with WT/ ddH_2O , and it was the same between those inoculated with TPS1^- and TPS2^- (Figure S1). Pairwise OPLS-DA was conducted between the extracts of wheat spikes inoculated with the TPS^- mutants and those inoculated with WT/ ddH_2O for both the resistant and susceptible wheat varieties. In addition, OPLS-DA modeling was also conducted comparing the extracts of wheat spikes inoculated with different TPS^- mutants. Significantly different metabolites between these two groups were tabulated in Table 1. OPLS-DA model parameters showed that for the FHB-resistant wheat Sumai 3, there were clear metabolic differences between being inoculated with mutants (including TPS1^- and TPS2^-) and with ddH_2O /WT (Figure 3). Significantly altered metabolites between the two groups were tabulated in Table 1. The loadings plots of OPLS-DA showed that compared with ddH_2O , inoculation with TPS1^- in the resistant wheat induced increased levels of Phe, uridine, guanosine, hypoxanthine, p-hydroxy cinnamic acid and chlorogenic acid together with a decreased level of α -ketoglutarate (Figure 3a, Table 1). Inoculation with TPS2^- in Sumai 3 led to higher levels for Phe, guanosine, p-hydroxy cinnamic acid, and chlorogenic acid along with a lower level of α -ketoglutarate than with ddH_2O , which was similar to inoculation with TPS1^- ; in addition, inoculation with TPS2^- also led to a decrease in phosphocholine level (Figure 3c, Table 1). Compared with WT, inoculation with TPS1^- in the FHB-resistant wheat resulted in elevated levels

of guanosine and thymidine together with reduced levels of myo-inositol, Ala, Asp, and glycine betaine (Figure 3b, Table 1). However, inoculation with *TPS2*⁻ in Sumai 3 led to increased thymidine level together with decreased levels of sucrose and myo-inositol (Figure 3d, Table 1). Furthermore, we compared the metabolic profiles for inoculation with the *TPS1*⁻ and *TPS2*⁻ mutants in the resistant wheat. The results indicated that there was no obvious metabolic difference between those inoculated with different *TPS*⁻ mutants ($R^2X = 0.636$, $Q^2 = 0.126$, CV-ANOVA $p = 1$).

For the susceptible wheat Annon 8455, OPLS-DA model parameters indicated that there were obvious metabolic differences between those inoculated with mutants (including *TPS1*⁻ and *TPS2*⁻) and with ddH₂O (Figure 4). The color loading plots of OPLS-DA revealed that compared with ddH₂O, infection with the *TPS1*⁻ mutant in the susceptible wheat induced increased levels of fumarate, glycine betaine, and adenosine (Figure 4a, Table 1). Infection with the *TPS2*⁻ mutant in Annon 8455 led to lower levels of sucrose, fumarate, α -ketoglutarate, phosphocholine, adenosine, guanosine, and thymidine (Figure 4b, Table 1). However, there were no significant metabolic differences between inoculation with *TPS1*⁻ and with WT ($R^2X = 0.868$, $Q^2 = 0.258$, CV-ANOVA $p = 1$) or between inoculation with *TPS2*⁻ and with WT ($R^2X = 0.769$, $Q^2 = 0.0965$, CV-ANOVA $p = 1$) in the susceptible wheat. The results also showed that for the susceptible wheat, compared with *TPS1*⁻, infection with *TPS2*⁻ resulted in a reduction in the levels of most metabolites including two sugars (glucose and fructose), Gln, three organic acids (fumarate, malate, and formate), two choline metabolites (glycine betaine and phosphocholine), and two nucleotide metabolites (adenosine and guanosine) (Figure 4c, Table 1).

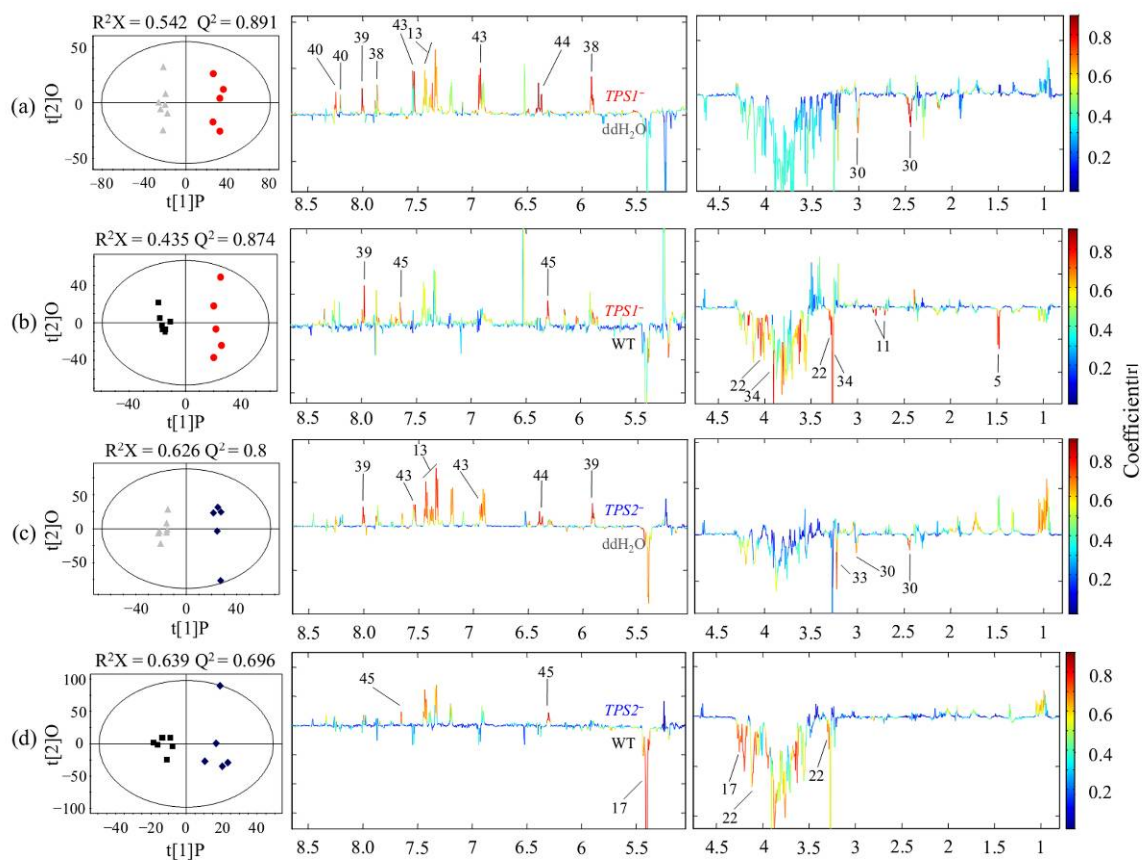


Figure 3. OPLS-DA scores plots (left) and coefficient-coded loadings plots (right) showing metabolic differences of FHB-resistant wheat Sumai 3 inoculated with (a) *TPS1*⁻ (red) vs. ddH₂O (grey) (CV-ANOVA $p = 0.0018$), (b) *TPS1*⁻ (red) vs. WT (black) (CV-ANOVA $p = 0.0029$), (c) *TPS2*⁻ (blue) vs. ddH₂O (grey) (CV-ANOVA $p = 0.014$), and (d) *TPS2*⁻ (blue) vs. WT (black) (CV-ANOVA $p = 0.01$). Metabolite keys are the same as in Figure 1 and Table S1.

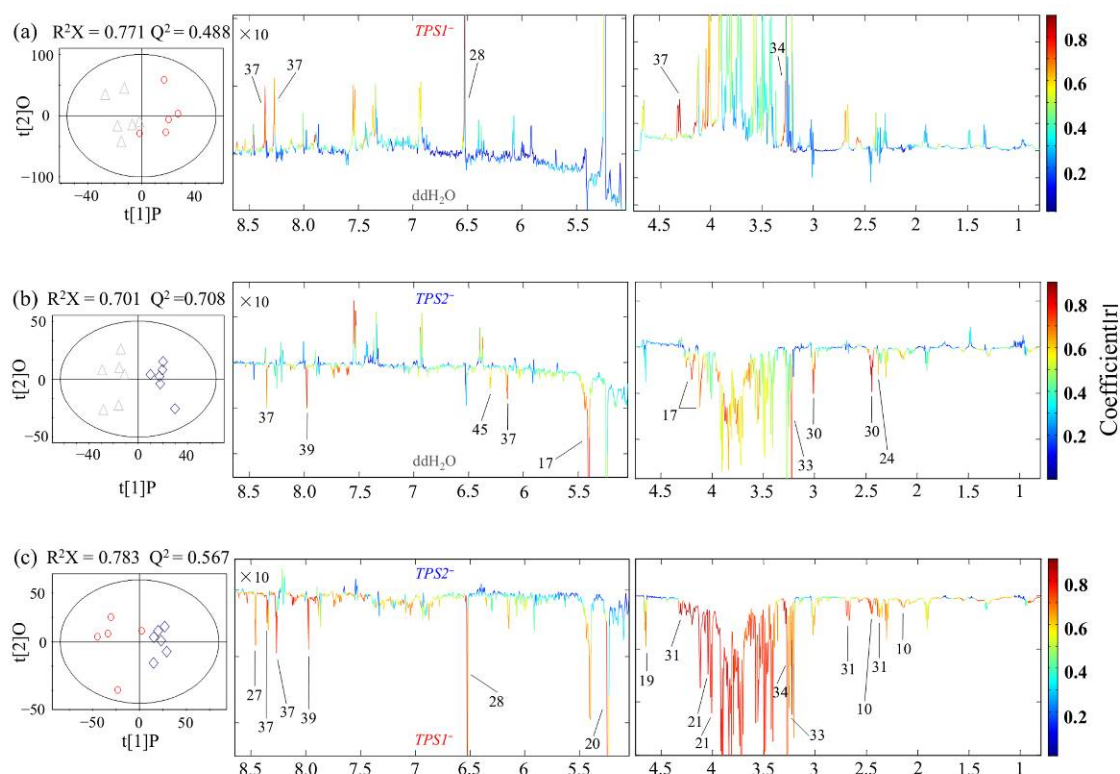


Figure 4. OPLS-DA scores plots (left) and coefficient-coded loadings plots (right) showing metabolic differences of FHB-susceptible wheat Annon 8455 inoculated with (a) *TPS1*[−] (red) vs. ddH₂O (grey) (CV-ANOVA $p = 0.005$), (b) *TPS2*[−] (blue) vs. ddH₂O (grey) (CV-ANOVA $p = 0.001$) and (c) *TPS2*[−] (blue) vs. *TPS1*[−] (red) (CV-ANOVA $p = 0.005$). Metabolite keys are the same as in Figure 1 and Table S1.

Table 1. Significantly changed metabolites in the resistant and susceptible wheat when inoculated with ddH₂O (H₂O), WT, *TPS1*[−], and *TPS2*[−].

Metabolites (No)	Coefficient (r) ^a						
	Sumai 3 (Resistant)			Annon 8455 (Susceptible)			
	<i>TPS1</i> [−] vs. H ₂ O	<i>TPS1</i> [−] vs. WT	<i>TPS2</i> [−] vs. H ₂ O	<i>TPS2</i> [−] vs. WT	<i>TPS1</i> [−] vs. H ₂ O	<i>TPS2</i> [−] vs. H ₂ O	<i>TPS2</i> [−] vs. <i>TPS1</i> [−]
Sugars							
sucrose (17) ^c				−0.849 ^b		−0.882	
α-glucose (18)							−0.826
β-glucose (19)							−0.816
fructose (21)							−0.857
myo-inositol (22)		−0.788		−0.821			
Amino acids							
Ala (5)		−0.781					
Gln (10)							−0.762
Asp (11)		−0.857					
Phe (13)	0.835		0.756				
Organic acids							
pyruvate (24)						−0.841	
formate (27)							−0.823
fumarate (28)					0.794		−0.904
a-KG (30)	−0.836		−0.782			−0.769	
malate (31)							−0.963
Choline metabolites							
phosphocholine (33)			−0.859			−0.877	−0.871
glycine betaine (34)		−0.837			0.814		−0.892

Table 1. Cont.

Metabolites (No)	Coefficient (r) ^a			
	Sumai 3 (Resistant)		Annong 8455 (Susceptible)	
Nucleotide metabolites				
adenosine (37)			0.824	−0.805
uridine (38)	0.825			−0.917
guanosine (39)	0.929	0.758	0.799	−0.826
hypoxanthine (40)	0.856			−0.799
thymidine (45)		0.821	0.834	−0.843
Secondary metabolites				
p-hydroxy cinnamic acid (43)	0.854		0.753	
chlorogenic acid (44)	0.922		0.826	

^a The coefficients were obtained from OPLS-DA results, and positive and negative signs indicate positive and negative correlation in the concentrations, respectively. ^b Positive and negative signs indicate the elevation and decrease of the metabolite levels. Values for $p \geq 0.05$ were not tabulated. ^c Metabolite keys are identical to those in Figure 1 and Table S1.

4. Discussion

FHB induced by *Fg* is a destructive disease for wheat. In our previous study [21], we obtained two mutants, *TPS1*[−] and *TPS2*[−], carrying a single deletion of *TPS1* (trehalose 6-phosphate synthase) and *TPS2* (trehalose 6-phosphate phosphatase), respectively, both of these two enzymes being involved in trehalose synthesis in *Fg*. Liu et al. also found that *Fg* *TPS1*[−] and *TPS2*[−] both produce fewer mycotoxins than WT (5035), and *TPS2*[−] produces fewer mycotoxins than *TPS1*[−] [22]. However, the metabolic responses of FHB-resistant and -susceptible wheat to *Fg* (WT, *TPS1*[−], and *TPS2*[−]) inoculation are not clear, but could give us metabolic information related to trehalose synthesis and FHB resistance.

Sumai 3 is a traditional FHB-resistant wheat variety, while Annong 8455 is a known FHB-susceptible wheat variety. The metabolic differences in both FHB-resistant and -susceptible wheat varieties when inoculated with *TPS*[−] and with ddH₂O could give us metabolic information about *Fg* pathogenicity, while the metabolic differences between inoculation with *TPS*[−] and with WT in both FHB-resistant and -susceptible wheat varieties could give us metabolic information about the difference in pathogenicity induced by *TPS1* and *TPS2* mutations.

For the resistant wheat Sumai 3, there were higher levels of Phe, guanosine, p-HCA and chlorogenic acid together with a lower level of α -KG after being inoculated with *TPS1*[−] or *TPS2*[−] when compared with being inoculated with ddH₂O (Figures 3 and 5, Table 1). This result indicated that Phe, p-HCA, and chlorogenic acid might be closely related to FHB-resistance. This is not surprising because both p-HCA and chlorogenic acid are secondary metabolites derived from the shikimate pathway for biosynthesis of phenylpropanoid and flavonoid metabolites. It has been reported that Sumai 3 has a fast and strong response primarily through the activation of the shikimate pathway [28]. HCAs have been reported to play roles in plant defense responses to pathogen challenge and wounding as integral components [46,47]. Chlorogenic acid, belonging to phenolic acids, has been reported to be a resistance factor to *Fg* in maize [48], to *Podosphaera* in miniature roses [49] and to *diatraea saccharalis* in sugarcane [50]. Sumai 3 might synthesize HCAs to reduce pathogen advancement through thickening host cell walls together with synthesizing antifungal/antioxidant chlorogenic acid for inhibiting pathogen growth, in turn reducing subsequent mycotoxin biosynthesis in *Fg* [51]. In a word, shikimate-mediated secondary metabolism was activated in the FHB-resistant wheat to produce HCAs and chlorogenic acid to inhibit the growth of *Fg* and reduce the production of mycotoxins.

5. Conclusions

In conclusion, when infected by *Fg*, FHB-susceptible and -resistant wheat showed different metabolic responses. Specifically, compared with ddH₂O, resistant wheat increased the levels of Phe, p-HCA, and chlorogenic acid to resist *TPS*[−] mutants; however, susceptible wheat did not. The metabolic difference might be caused by trehalose deletion and redundancy of T6P in the susceptible wheat when infected by *TPS1*[−] or *TPS2*[−] compared with ddH₂O. Finally, a hypothesis is proposed that when infected by *Fg*, shikimate-mediated secondary metabolism was activated in the FHB-resistant wheat to produce HCAs and chlorogenic acid to inhibit the growth of *Fg* and reduce the production of mycotoxins. However, it should be stressed that the molecular relationships between the trehalose biosynthetic pathway in *Fg* and shikimate-mediated secondary metabolism in wheat remains to be further studied.

Supplementary Materials: The following supporting information can be downloaded at: <https://www.mdpi.com/article/10.3390/metabo12080727/s1>, Table S1. Assignment of NMR data for metabolites in FHB-resistant (Sumai 3) and -susceptible (Annong 8455) wheat varieties inoculated with ddH₂O, wild type (WT), *TPS1*[−] and *TPS2*[−]; Figure S1. PCA scores plots of the NMR data for FHB-resistant Sumai 3 (a) and -susceptible wheat Annong 8455 (b). The numbers in parentheses indicate the overall variance explained in the first two principal components. Grey (triangle), black (square), red (circle), and blue (diamond) indicate metabolites in both FHB-resistant (solid symbol) and -susceptible wheat (open symbol) inoculated with ddH₂O, WT, *TPS1*[−], and *TPS2*[−], respectively.

Author Contributions: Conceptualization, X.Z. and C.L.; methodology, H.L.; software, L.L. and X.F.; validation, X.Z., C.L. and F.C.; formal analysis, X.F.; investigation, X.Z.; resources, X.Z.; data curation, L.L.; writing—original draft preparation, C.L.; writing—review and editing, F.C. and D.Z.; visualization, C.L.; supervision, X.Z.; project administration, X.Z.; funding acquisition, X.Z. All authors have read and agreed to the published version of the manuscript.

Funding: This research was funded by National Natural Science Foundation of China (32071990, 21991081 and 21735007), the National Key R&D Program of China (2018YFE0202300), and the Interdisciplinary Cultivation Project of the Innovation Academy for Precision Measurement of Science and Technology (S21S1101) and The APC was funded by the National Key R&D Program of China (2018YFE0202300).

Institutional Review Board Statement: Not applicable.

Informed Consent Statement: Not applicable.

Data Availability Statement: Not applicable.

Conflicts of Interest: All authors declared no conflict of interest.

References

1. Blanco, A.; Bellomo, M.; Cenci, A.; De Giovanni, C.; D'ovidio, R.; Iacono, E.; Laddomada, B.; Pagnotta, M.; Porceddu, E.; Sciancalepore, A. A genetic linkage map of durum wheat. *Theor. Appl. Genet.* **1998**, *97*, 721–728. [[CrossRef](#)]
2. Otto, C.; Kianian, S.; Elias, E.; Stack, R.; Joppa, L. Genetic dissection of a major Fusarium head blight QTL in tetraploid wheat. *Plant Mol. Biol.* **2002**, *48*, 625–632. [[CrossRef](#)] [[PubMed](#)]
3. Duffeck, M.R.; Bandara, A.Y.; Weerasooriya, D.K.; Collins, A.A.; Jensen, P.J.; Kuldau, G.A.; Del Ponte, E.M.; Esker, P.D. Fusarium head blight of small grains in pennsylvania: Unravelling species diversity, toxin types, growth, and triazole sensitivity. *Phytopathology* **2022**, *112*, 794–802. [[CrossRef](#)] [[PubMed](#)]
4. Podgorska-Kryszczuk, I.; Solarska, E.; Kordowska-Wiater, M. Reduction of the fusarium mycotoxins: Deoxynivalenol, nivalenol and zearalenone by selected non-conventional yeast strains in wheat grains and bread. *Molecules* **2022**, *27*, 1578. [[CrossRef](#)]
5. Goswami, R.S.; Kistler, H.C. Heading for disaster: *Fusarium graminearum* on cereal crops. *Mol. Plant Pathol.* **2004**, *5*, 515–525. [[CrossRef](#)]
6. Xu, X.-M.; Parry, D.; Nicholson, P.; Thomsett, M.; Simpson, D.; Edwards, S.; Cooke, B.; Doohan, F.; Brennan, J.; Moretti, A. Predominance and association of pathogenic fungi causing Fusarium ear blight in wheat in four European countries. *Eur. J. Plant Pathol.* **2005**, *112*, 143–154. [[CrossRef](#)]
7. Rudd, J.; Horsley, R.; McKendry, A.; Elias, E. Host plant resistance genes for Fusarium head blight. *Crop Sci.* **2001**, *41*, 620–627. [[CrossRef](#)]

8. Avonce, N.; MendozaVargas, A.; Morett, E.; Iturriaga, G. Insights on the evolution of trehalose biosynthesis. *BMC Evol. Biol.* **2006**, *6*, 109. [[CrossRef](#)]
9. Gancedo, C.; Flores, C.L. The importance of a functional trehalose biosynthetic pathway for the life of yeasts and fungi. *FEMS Yeast Res.* **2004**, *4*, 351–359. [[CrossRef](#)]
10. Purvis, J.E.; Yomano, L.; Ingram, L. Enhanced trehalose production improves growth of *Escherichia coli* under osmotic stress. *Appl. Environ. Microb.* **2005**, *71*, 3761–3769. [[CrossRef](#)]
11. Crowe, J.H.; Crowe, L.M.; Chapman, D. Preservation of membranes in anhydrobiotic organisms: The role of trehalose. *Science* **1984**, *223*, 701–703. [[CrossRef](#)] [[PubMed](#)]
12. Singer, M.A.; Lindquist, S. Multiple effects of trehalose on protein folding in vitro and in vivo. *Mol. Cell* **1998**, *1*, 639–648. [[CrossRef](#)]
13. Cao, Y.; Wang, Y.; Dai, B.; Wang, B.; Zhang, H.; Zhu, Z.; Xu, Y.; Cao, Y.; Jiang, Y.; Zhang, G. Trehalose is an important mediator of Cap1p oxidative stress response in *Candida albicans*. *Biol. Pharm. Bull.* **2008**, *31*, 421–425. [[CrossRef](#)]
14. Zakharova, K.; Tesei, D.; Marzban, G.; Dijksterhuis, J.; Wyatt, T.; Sterflinger, K. Microcolonial fungi on rocks: A life in constant drought? *Mycopathologia* **2013**, *175*, 537–547. [[CrossRef](#)]
15. Zhang, Z.W.; Sun, M.; Gao, Y.M.; Luo, Y. Exogenous trehalose differently improves photosynthetic carbon assimilation capacities in maize and wheat under heat stress. *J. Plant Interact.* **2022**, *17*, 361–370. [[CrossRef](#)]
16. Elbein, A.D.; Pan, Y.; Pastuszak, I.; Carroll, D. New insights on trehalose: A multifunctional molecule. *Glycobiology* **2003**, *13*, 17–27. [[CrossRef](#)]
17. Bell, W.; Klaassen, P.; Ohnacker, M.; Boller, T.; Herweijer, M.; Schoppink, P.; Vanderzee, P.; Wiemken, A. Characterization of the 56-kDa subunit of yeast trehalose-6-phosphate synthase and cloning of its gene reveal its identity with the product of CIF1, a regulator of carbon catabolite inactivation. *FEBS J.* **1992**, *209*, 951–959. [[CrossRef](#)]
18. Vuorio, O.E.; Kalkkinen, N.; Londesborough, J. Cloning of two related genes encoding the 56-kDa and 123-kDa subunits of trehalose synthase from the yeast *Saccharomyces cerevisiae*. *FEBS J.* **1993**, *216*, 849–861. [[CrossRef](#)]
19. Al-Bader, N.; Vanier, G.; Liu, H.; Gravelat, F.N.; Urb, M.; Hoareau, C.M.-Q.; Campoli, P.; Chabot, J.; Filler, S.G.; Sheppard, D.C. Role of trehalose biosynthesis in *Aspergillus fumigatus* development, stress response, and virulence. *Infect. Immun.* **2010**, *78*, 3007–3018. [[CrossRef](#)]
20. Puttikamonkul, S.; Willger, S.D.; Grahl, N.; Perfect, J.R.; Movahed, N.; Bothner, B.; Park, S.; Paderu, P.; Perlin, D.S.; Cramer, R.A., Jr. Trehalose 6-phosphate phosphatase is required for cell wall integrity and fungal virulence but not trehalose biosynthesis in the human fungal pathogen *Aspergillus fumigatus*. *Mol. Microbiol.* **2010**, *77*, 891–911. [[CrossRef](#)]
21. Song, X.-S.; Li, H.-P.; Zhang, J.-B.; Song, B.; Huang, T.; Du, X.-M.; Gong, A.-D.; Liu, Y.-K.; Feng, Y.-N.; Agboola, R.S. Trehalose 6-phosphate phosphatase is required for development, virulence and mycotoxin biosynthesis apart from trehalose biosynthesis in *Fusarium graminearum*. *Fungal Genet. Biol.* **2014**, *63*, 24–41. [[CrossRef](#)] [[PubMed](#)]
22. Liu, C.; Chen, F.; Zhang, J.; Liu, L.; Lei, H.; Li, H.; Wang, Y.; Liao, Y.-C.; Tang, H. Metabolic changes of *Fusarium graminearum* induced by TPS gene deletion. *J. Proteome Res.* **2019**, *18*, 3317–3327. [[CrossRef](#)] [[PubMed](#)]
23. Chen, F.; Liu, C.; Zhang, J.; Lei, H.; Li, H.-P.; Liao, Y.-C.; Tang, H. Combined metabolomic and quantitative RT-PCR analyses revealed metabolic reprogramming associated with *Fusarium graminearum* resistance in transgenic *Arabidopsis thaliana*. *Front. Plant Sci.* **2017**, *8*, 2177. [[CrossRef](#)] [[PubMed](#)]
24. Liu, C.X.; Ding, F.; Hao, F.H.; Yu, M.; Lei, H.H.; Wu, X.Y.; Zhao, Z.X.; Guo, H.X.; Yin, J.; Wang, Y.L.; et al. Reprogramming of seed metabolism facilitates pre-harvest sprouting resistance of wheat. *Sci. Rep.* **2016**, *6*, 20593. [[CrossRef](#)] [[PubMed](#)]
25. Liu, C.; Hao, F.; Hu, J.; Zhang, W.; Wan, L.; Zhu, L.; Tang, H.; He, G. Revealing different systems responses to brown planthopper infestation for pest susceptible and resistant rice plants with the combined metabolomic and gene-expression analysis. *J. Proteome Res.* **2010**, *9*, 6774–6785. [[CrossRef](#)]
26. Marti, G.; Erb, M.; Bocard, J.; Glauser, G.; Doyen, G.R.; Villard, N.; Robert, C.A.M.; Turlings, T.C.; Rudaz, S.; Wolfender, J.L. Metabolomics reveals herbivore-induced metabolites of resistance and susceptibility in maize leaves and roots. *Plant Cell Environ.* **2013**, *36*, 621–639. [[CrossRef](#)]
27. Freitas, D.D.; Carlos, E.F.; Gil, M.C.S.D.; Vieira, L.G.E.; Alcantara, G.B. NMR-based metabolomic analysis of huanglongbing-asymptomatic and -symptomatic citrus trees. *J. Agric. Food Chem.* **2015**, *63*, 7582–7588. [[CrossRef](#)]
28. Cuperlovic-Culf, M.; Wang, L.; Forseille, L.; Boyle, K.; Merkley, N.; Burton, I.; Fobert, P.R. Metabolic biomarker panels of response to fusarium head blight infection in different wheat varieties. *PLoS ONE* **2016**, *11*, e0153642. [[CrossRef](#)]
29. Baldaccicresp, F.; Chang, C.; Mickaël Maucourt Deborde, C.; Hopkins, J.; Lecomte, P. (Homo) glutathione deficiency impairs root-knot nematode development in *Medicago truncatula*. *PLoS Pathog.* **2012**, *8*, e1002471.
30. Kumar, Y.; Zhang, L.; Panigrahi, P.; Dholakia, B.B.; Dewangan, V.; Chavan, S.G.; Kunjir, S.M.; Wu, X.; Li, N.; Rajmohan, P.R. *Fusarium oxysporum* mediates systems metabolic reprogramming of chickpea roots as revealed by a combination of proteomics and metabolomics. *Plant Biotechnol. J.* **2016**, *14*, 1589–1603. [[CrossRef](#)]
31. Marentes-Culma, R.; Cuellar-Cuestas, C.; Ardila, H.D.; Coy-Barrera, E. 5- n -alkylresorcinol-based metabolic response of rice to the interaction with burkholderia glumae: A chemical characterization of the temporal and spatial variations depending on environmental conditions. *J. Plant Interact.* **2022**, *17*, 127–139. [[CrossRef](#)]
32. Liu, C.; Du, B.; Hao, F.; Lei, H.; Wan, Q.; He, G.; Wang, Y.; Tang, H. Dynamic metabolic responses of brown planthoppers towards susceptible and resistant rice plants. *Plant Biotechnol. J.* **2017**, *15*, 1346–1357. [[CrossRef](#)] [[PubMed](#)]

33. Zhang, Q.; Li, T.; Gao, M.; Ye, M.; Lin, M.; Wu, D.; Guo, J.; Guan, W.; Wang, J.; Yang, K.; et al. Transcriptome and metabolome profiling reveal the resistance mechanisms of rice against brown planthopper. *Int. J. Mol. Sci.* **2022**, *23*, 4083. [[CrossRef](#)] [[PubMed](#)]
34. Browne, R.A.; Brindle, K.M. ¹H NMR-based metabolite profiling as a potential selection tool for breeding passive resistance against Fusarium head blight (FHB) in wheat. *Mol. Plant Pathol.* **2007**, *8*, 401–410. [[CrossRef](#)] [[PubMed](#)]
35. Miao, Y.; Xu, L.; He, X.; Zhang, L.; Shaban, M.; Zhang, X.; Zhu, L. Suppression of tryptophan synthase activates cotton immunity by triggering cell death via promoting SA synthesis. *Plant J.* **2019**, *98*, 329–345. [[CrossRef](#)] [[PubMed](#)]
36. Zhang, J.B.; Li, H.P.; Dang, F.J.; Qu, B.; Xu, Y.B.; Zhao, C.S.; Liao, Y.C. Determination of the trichothecene mycotoxin chemotypes and associated geographical distribution and phylogenetic species of the *Fusarium graminearum* clade from China. *Mycol. Res.* **2007**, *111*, 967–975. [[CrossRef](#)]
37. Wu, A.B.; Li, H.P.; Zhao, C.S.; Liao, Y.C. Comparative pathogenicity of *Fusarium graminearum* isolates from China revealed by wheat coleoptile and floret inoculations. *Mycopathologia* **2005**, *160*, 75–83. [[CrossRef](#)]
38. Duvick, J.; Rood, T.; Rao, A.G.; Marshak, D.R. Purification and characterization of a novel antimicrobial peptide from maize (*Zea mays* L.) kernels. *J. Biol. Chem.* **1992**, *267*, 18814–18820. [[CrossRef](#)]
39. Li, X.; Zhang, J.; Song, B.; Li, H.; Xu, H.; Qu, B.; Dang, F.; Liao, Y. Resistance to Fusarium head blight and seedling blight in wheat is associated with activation of a cytochrome P450 gene. *Phytopathology* **2010**, *100*, 183–191. [[CrossRef](#)]
40. Wu, X.Y.; Li, N.; Li, H.D.; Tang, H.R. An optimized method for NMR-based plant seed metabolomic analysis with maximized polar metabolite extraction efficiency, signal-to-noise ratio, and chemical shift consistency. *Analyst* **2014**, *139*, 1769–1778. [[CrossRef](#)]
41. Trygg, J.; Wold, S. Orthogonal projections to latent structures (O-PLS). *J. Chemometr.* **2002**, *16*, 119–128. [[CrossRef](#)]
42. Eriksson, L.; Trygg, J.; Wold, S. CV-ANOVA for significance testing of PLS and OPLS® models. *J. Chemometr.* **2008**, *22*, 594–600. [[CrossRef](#)]
43. Cloarec, O.; Dumas, M.E.; Trygg, J.; Craig, A.; Barton, R.H.; Lindon, J.C.; Nicholson, J.K.; Holmes, E. Evaluation of the orthogonal projection on latent structure model limitations caused by chemical shift variability and improved visualization of biomarker changes in ¹H NMR spectroscopic metabolomic studies. *Anal. Chem.* **2005**, *77*, 517–526. [[CrossRef](#)] [[PubMed](#)]
44. Fan, T.W.M. Metabolite profiling by one-and two-dimensional NMR analysis of complex mixtures. *Prog. Nucl. Mag. Res. Spectrosc.* **1996**, *28*, 161–219. [[CrossRef](#)]
45. Fan, T.W.M.; Lane, A.N. Structure-based profiling of metabolites and isotopomers by NMR. *Prog. Nucl. Mag. Res. Spectrosc.* **2008**, *52*, 69–117. [[CrossRef](#)]
46. Facchini, P.J.; Hagel, J.; Zulak, K.G. Hydroxycinnamic acid amide metabolism: Physiology and biochemistry. *Can. J. Bot.-Rev. Can. Bot.* **2002**, *80*, 577–589. [[CrossRef](#)]
47. González-Lamothe, R.; Mitchell, G.; Gattuso, M.; Diarra, M.S.; Malouin, F.; Bouarab, K. Plant antimicrobial agents and their effects on plant and human pathogens. *Int. J. Mol. Sci.* **2009**, *10*, 3400–3419. [[CrossRef](#)]
48. Atanasova-Penichon, V.; Pons, S.; Pinson-Gadais, L.; Picot, A.; Marchegay, G.; Bonnin-Verdal, M.-N.; Ducos, C.; Barreau, C.; Roucolle, J.; Sehabiague, P. Chlorogenic acid and maize ear rot resistance: A dynamic study investigating *Fusarium graminearum* development, deoxynivalenol production, and phenolic acid accumulation. *Mol. Plant-Microbe Interact.* **2012**, *25*, 1605–1616. [[CrossRef](#)]
49. Shetty, R.; Fretté, X.; Jensen, B.; Shetty, N.P.; Jensen, J.D.; Jorgensen, H.J.L.; Newman, M.-A.; Christensen, L.P. Silicon-induced changes in antifungal phenolic acids, flavonoids, and key phenylpropanoid pathway genes during the interaction between *Miniature roses* and the biotrophic pathogen *Podosphaera pannosa*. *Plant Physiol.* **2011**, *157*, 2194–2205. [[CrossRef](#)]
50. Sabino, A.R.; Tavares, S.S.; Riffel, A.; Li, J.V.; Oliveira, D.J.; Feres, C.I.; Henrique, L.; Oliveira, J.S.; Correia, G.D.; Sabino, A.R.; et al. ¹H NMR metabolomic approach reveals chlorogenic acid as a response of sugarcane induced by exposure to diatraea saccharalis. *Ind. Crops Prod.* **2019**, *140*, 111651. [[CrossRef](#)]
51. Gunnaiah, R.; Kushalappa, A.C. Metabolomics deciphers the host resistance mechanisms in wheat cultivar Sumai-3, against trichothecene producing and non-producing isolates of *Fusarium graminearum*. *Plant Physiol. Biochem.* **2014**, *83*, 40–50. [[CrossRef](#)] [[PubMed](#)]
52. Arisan-Atac, I.; Wolschek, M.F.; Kubicek, C.P. Trehalose-6-phosphate synthase A affects citrate accumulation by *Aspergillus niger* under conditions of high glycolytic flux. *FEMS Microbiol. Lett.* **1996**, *140*, 77–83. [[CrossRef](#)] [[PubMed](#)]